LOCAL BUCKLING ANALYSIS OF PULTRUDED FRP PROFILES: A MECHANICAL MODEL

L. Ascione[1], V. P. Berardi[1*], A. Giordano[1], S. Spadea[1]

[1]*Department of Civil Engineering, University of Salerno*
**berardi@unisa.it*

Keywords: buckling, thin walled beams, composite materials, finite element analysis.

Abstract

A mechanical model capable to predict the local buckling of pultruded FRP thin-walled beams and columns, taking into account the shear deformability of composite materials, is presented in this paper. The model is based on the individual analysis of buckling of the components of FRP profile, assumed as elastically restrained transversely isotropic plates. The analysis is developed within the field of small strains and moderate rotations.

1 Introduction

The use of pultruded Fiber Reinforced Polymers (FRP) thin walled beams represents an interesting challenge in the field of Civil Engineering, in view of the advantages that composite materials exhibit in comparison with conventional ones.

The mechanical behavior of these structural elements is strongly influenced by buckling phenomena [1-3], due to their thin-walled sectional geometry and the low shear stiffness of composite materials. In fact, several studies have shown that shear deformation can significantly affect the ultimate failure of thin-walled FRP members [4-7]. With reference to local buckling, in agreement with Italian guidelines for designing structures entirely made of composite materials [8], the analysis of thin walled FRP shapes can be accomplished by modeling individually the profile plate components (i.e. flanges and web in the case of open section), under the assumption of flexible plate junctions (i.e. flange-web junctions in the case of open section) [9-11].

This work presents a mechanical model able to predict the local buckling of pultruded FRP thin-walled beams and columns, taking into account the shear deformability of composites. With the aim of performing a buckling analysis of the single component of FRP profile, assumed as elastically restrained plates, Mindlin-Reissner theory is developed in the field of small strains and moderate rotations and is extended to elastic transversely isotropic materials. The numerical analysis here presented, performed on the basis of a weak formulation of the buckling problem within finite element method, examines the case of an ‘‘I’’ simply supported beam subject to transverse loads.

2 Kinematics

Let consider an “I” beam with the constant cross-section of Figure 1. The adopted Cartesian reference frame has the origin in the centroid, *G*, of one of the bases of the beam, being the *X* and *Y* axes coincident with the central axes of inertia of the cross-section and the *Z* axis coincident with the longitudinal beam axis.

The cross-section can be divided into five plate components, internally connected through flexible flange-web junctions (Figure 1).

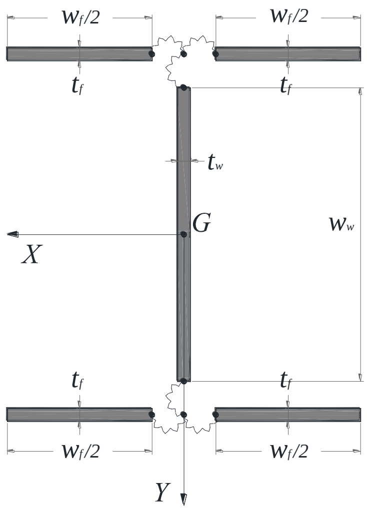

Figure 1. Schematic representation of the pultruded profile cross section.

Then, the single plate can be modeled as an elastically restrained transversely isotropic one.
Let us denote the undeformed mid-plane of the plate with the symbol Ω_0. The total domain of the plate is $\Omega_0 \times (-h/2, +h/2)$. The boundary of the total domain consists of surfaces $S^+(z = +h/2)$, $S^-(z = -h/2)$ and $\Gamma = \partial\Omega_0 \times (-h/2, +h/2)$ (Figure 2). Γ is a curved surface, with outwards normal $\hat{\mathbf{n}} = n_x \hat{\mathbf{e}}_\mathbf{x} + n_y \hat{\mathbf{e}}_y$, where n_x and n_y are the direction cosines of the unit normal.
The classical theory available for shear deformable plates, due to Mindlin and Reissner [12]-[13], is based on the following assumptions: a) straight lines perpendicular to the mid-plane (i.e. transverse normals) before deformation remain straight after deformations; b) the transverse normals do not experience elongation.

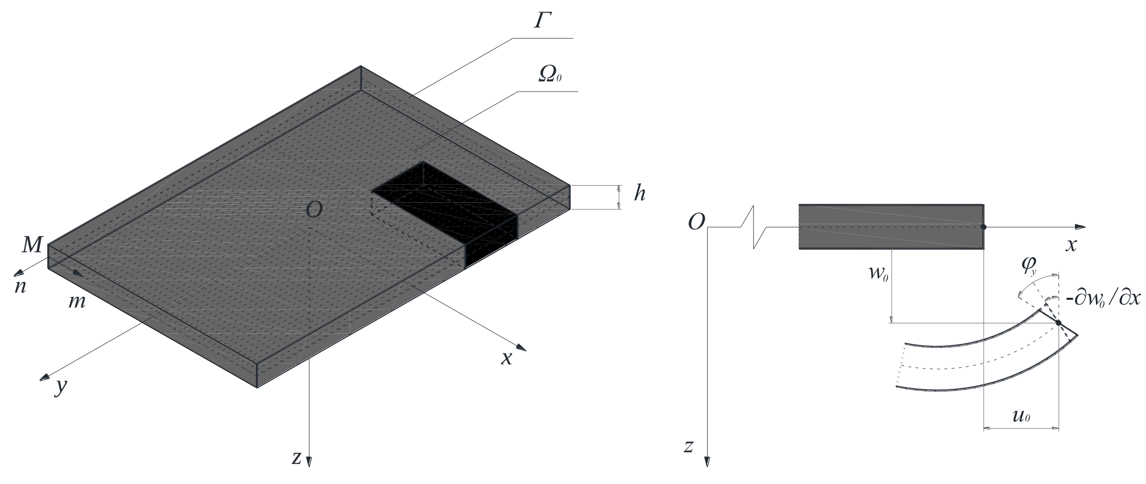

Figure 2. a) Global $\{O, x, y, z\}$ and local $\{M, m, n, z\}$ coordinate system of the plate;
b) undeformed and deformed geometry of the shear deformable plate.

Therefore, the displacement field of the plate, referred to the reference system $\{O, x, y, z\}$ (Figure 2), can be written in the following form:

$$u = u(x, y, z) = u_0(x, y) + \varphi_y(x, y) \cdot z\,, \tag{1a}$$
$$v = v(x, y, z) = v_0(x, y) - \varphi_x(x, y) \cdot z\,, \tag{1b}$$
$$w = w(x, y) = w_0(x, y)\,, \tag{1c}$$

where (u_0, v_0, w_0) denote the displacements of a material point at the mid-plane of the plate and (φ_x, φ_y) are the rotations of transverse normals about the x-axis and y-axis, respectively.

According to the hypothesis of small strains accompanied by moderate rotation and assuming that ω_{xy} infinitesimal rotation tensor component is negligible, it is easy to show that the column vector, $\bar{}$, associated with Green–Saint Venant strain tensor assume the following expression:

$$\bar{\mathbf{E}} = {}^{(1)} + {}^{(2)} = {}^{(1c)} + z\,{}^{(1l)} + {}^{(2)}, \tag{2a}$$

$$\begin{pmatrix} \bar{E}_{xx} \\ \bar{E}_{yy} \\ \bar{E}_{zz} \\ \bar{E}_{yz} \\ \bar{E}_{xz} \\ \bar{E}_{xy} \end{pmatrix} = \begin{pmatrix} 0 \\ 0 \\ 0 \\ \left(-\varphi_x + \dfrac{\partial w_0}{\partial y}\right) \\ \left(\varphi_y + \dfrac{\partial w_0}{\partial x}\right) \\ 0 \end{pmatrix} + z \begin{pmatrix} \dfrac{\partial \varphi_y}{\partial x} \\ -\dfrac{\partial \varphi_x}{\partial y} \\ 0 \\ 0 \\ 0 \\ \left(\dfrac{\partial \varphi_y}{\partial y} - \dfrac{\partial \varphi_x}{\partial x}\right) \end{pmatrix} + \begin{pmatrix} \dfrac{1}{8}\left(\varphi_y - \dfrac{\partial w_0}{\partial x}\right)^2 \\ \dfrac{1}{8}\left(\varphi_x + \dfrac{\partial w_0}{\partial y}\right)^2 \\ \dfrac{1}{8}\left[\left(\varphi_x + \dfrac{\partial w_0}{\partial y}\right)^2 + \left(\varphi_y - \dfrac{\partial w_0}{\partial x}\right)^2\right] \\ 0 \\ 0 \\ -\dfrac{1}{4}\left(\varphi_x + \dfrac{\partial w_0}{\partial y}\right)\left(\varphi_y - \dfrac{\partial w_0}{\partial x}\right) \end{pmatrix}, \tag{2b}$$

being ${}^{(1c)}$ the first order constant strain vectors, $z \cdot {}^{(1l)}$ the first order linear strain vector and ${}^{(2)}$ the second order strain vector.

3 Buckling Analysis

In order to analyze buckling behavior of shear deformable elastic plates, the following displacement field, responsible for the transition from fundamental configuration to varied one, is considered:

$$\Delta u(x, y, z) = \Delta \varphi_y(x, y) \cdot z\,, \tag{3a}$$
$$\Delta v(x, y, z) = -\Delta \varphi_x(x, y) \cdot z\,, \tag{3b}$$
$$\Delta w(x, y) = \Delta w_0(x, y)\,. \tag{3c}$$

Thus, for small strains and moderate rotations, the strain-displacement relations take the form:

$$\Delta \bar{\mathbf{E}} = \Delta\,{}^{(1)} + \Delta\,{}^{(2)} = \Delta\,{}^{(1c)} + z\Delta\,{}^{(1l)} + \Delta\,{}^{(2)}\,. \tag{4}$$

The fundamental configuration and the corresponding total potential energy are indicated by C^0 and E^0, respectively, whereas the symbols C^* and E^* indicate the varied configuration and the corresponding total potential energy, respectively.

The equilibrium conditions in the configurations C^0 and C^* can be expressed in a variational form by equating to zero the first variations of the corresponding total potential energy functionals E^0 and E^*. Starting from these conditions, the following equation can be obtained:

$$\delta\left(\mathrm{E}^* - \mathrm{E}^0\right) = \delta\Delta\mathrm{E} = 0\,. \tag{5}$$

The hypothesis of small strains, available in the fundamental configuration, allows to express Eq. (5) in the form:

$$\delta\left(U - V_2 + V_2^*\right) = 0\,. \tag{6}$$

The term U is the elastic energy corresponding to the transition C^0 to C^* and the terms V_2 and V_2^* are, respectively, the second-order work carried out by the external forces and by the stresses acting in the fundamental configuration, when the plate configuration changes from C^0 to C^* [14].
On the basis of the results previously obtained, the expression of the elastic energy for a plate with rotational restraints along the sides parallel to *x* axis can be written as:

$$U = \frac{1}{2}\int_\Omega \int_{-h/2}^{+h/2} A_{ij}\Delta\varepsilon_i^{(1)}\Delta\varepsilon_j^{(1)}\, dz d\Omega + \frac{1}{2}\int_{-L_x/2}^{+L_x/2}\left[k^-\left(\Delta\varphi_x\big|_{y=-L_y/2}\right)^2 + k^+\left(\Delta\varphi_x\big|_{y=+L_y/2}\right)^2\right]dx. \tag{7}$$

In Eq. (7) k^- and k^+ represent the rotational spring stiffnesses (Figure 3) and there are:

$$\begin{aligned} &A_{44} = \frac{h^3}{12}\left(\frac{E_x}{1-\nu_{xy}^2 E_y/E_x}\right), A_{45} = \frac{h^3}{12}\left(\frac{\nu_{xy}E_y}{1-\nu_{xy}^2 E_y/E_x}\right), A_{55} = \frac{h^3}{12}\left(\frac{E_y}{1-\nu_{xy}^2 E_y/E_x}\right), \\ &A_{66} = \frac{h^3}{12}G_{xy},\; A_{77} = \chi_x h G_{yz}, A_{88} = \chi_y h G_{xy}, \end{aligned} \tag{8}$$

being E_x, E_y, ν_{xy}, G_{xy}, G_{yz} the independent elastic parameters, χ_x and χ_y the shear factors in *x* and *y* direction, respectively.
Since the applied loads do not work for the second order displacement responsible for the transition from configuration C^0 to C^*, the second-order work carried out by external forces, V_2, is zero.
The second-order work, V_2^*, carried out by stresses in the fundamental equilibrium configuration can be written as follows:

$$V_2^* = \lambda\int_\Omega \int_{-h/2}^{+h/2} \sigma_i^0 \Delta\varepsilon_i^{(2)}\, dz\, d\Omega\;. \tag{9}$$

In Eq. (9) λ is a constant by which the external loads must be multiplied to cause buckling, $\boldsymbol{\sigma}^{\mathbf{0}} = \left(N_x^0 \quad N_y^0 \quad N_{xy}^0\right)^T$ is the column vector associated with the Piola-Kirchhoff tensor (where $N_x^0 \quad N_y^0 \quad N_{xy}^0$ are the normal forces per unit length in the fundamental equilibrium configuration).

4 Finite element discretization

In order to apply the finite element method the mid-plane of the plate is subdivided in rectangular elements (Figure 3).

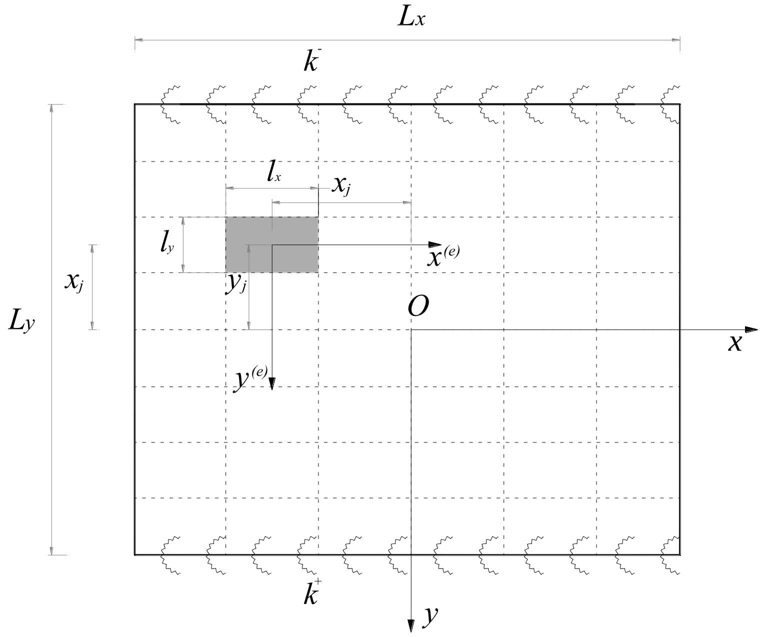

Figure 3. Discretization of the domain.

Assuming a quadratic 9-node Lagrange finite element, the above introduced displacements are independently interpolated as follows:

$$\Delta w_0^{(e)} = \sum_{i=1}^{9} \psi_i(\xi,\eta)\Delta w_{0i}^{(e)} \ , \ \Delta\varphi_x^{(e)} = \sum_{i=1}^{9} \psi_i(\xi,\eta)\Delta\varphi_{xi}^{(e)} \ , \ \Delta\varphi_y^{(e)} = \sum_{i=1}^{9} \psi_i(\xi,\eta)\Delta\varphi_{yi}^{(e)} \ , \qquad (10)$$

where $\psi_i(\xi,\eta)$ are the nine lagrangian quadratic shape functions [15]; $\Delta w_{0i}^{(e)}$, $\Delta\varphi_{xi}^{(e)}$ and $\Delta\varphi_{yi}^{(e)}$ represent the displacement components of the *i*-th node of the *e*-th finite element.
Starting from the FEM approach, the proposed model has been validated by comparing the theoretical prediction of buckling of an elastically restrained isotropic plate with the results reported in [16].

5 The case of a simply supported beam subject to a transverse load

Let us consider an ‘‘I’’ beam with torsional restrains at the ends and subject to a uniformly distributed transverse load, applied to its upper flange, as shown in Figure 4.

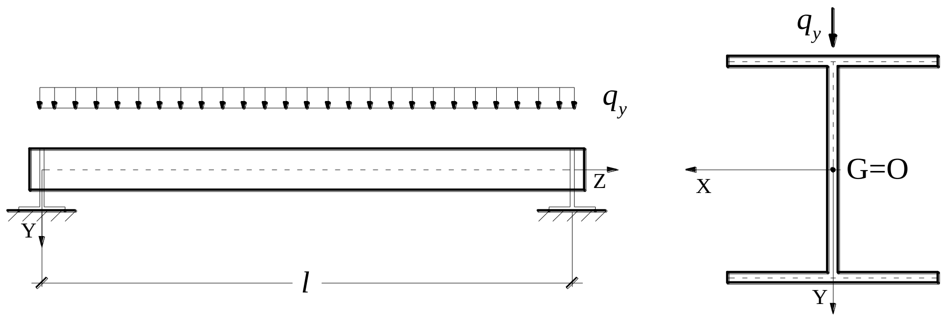

Figure 4. Load condition.

The normal forces per unit length, in the fundamental equilibrium configuration, are given by the following relationships, for the web:

$$N_x^0 = q\frac{\left(l\cdot x - x^2\right)y}{2I_x}t_w;\; N_y^0 = q\left(\frac{1}{2}+\frac{3}{2}\frac{y}{w_w}-2\frac{y^3}{{w_w}^3}\right); \tag{11a}$$

$$N_{xy}^0 = -\frac{q}{I_x}\left(\frac{l}{2}-x\right)\left[\left(\frac{{w_w}^2}{4}-y^2\right)t_w + S_f\right]; \tag{11b}$$

and the flange:

$$N_x^0 = q\frac{\left(l\cdot x - x^2\right)w_w}{4I_x}t_f;\; N_y^0 = 0;\; N_{xy}^0 = -\frac{q}{2I_x}\left(\frac{l}{2}-x\right)\left(\frac{w_f}{4}-y\right)t_f\cdot w_w. \tag{12}$$

In the previous equations S_f is the static moment of the flange about the *X* axis and I_x is the moment of inertia about *X* axis of the beam cross-section.
The boundary conditions for the web and the half flange are reported in Table 1.

Web	**Half Flange**
$\Delta w_0(x, y=\pm L_y/2) = \Delta w_0(x=\pm L_x/2, y) = 0$	$\Delta w_0(x, y=-L_y/2) = \Delta w_0(x=\pm L_x/2, y) = 0$
$\Delta\varphi_x(x=\pm L_x/2, y) = 0$	$\Delta\varphi_x(x=\pm L_x/2, y) = 0$
$\Delta\varphi_y(x, y=\pm L_y/2) = 0$	$\Delta\varphi_y(x, y=-L_y/2) = 0$
$k^- = k^+ = 0$	$k^- = k^+ = 0$

Table 1. Boundary conditions.

A parametric study is performed in order to investigate the buckling behavior of some pultruded GFRP (Glass Fiber Reinforced Polymer) “I’’ simply supported beams, characterized by fixed mechanical properties and different geometry, as listed in Table 2.

Beam	w_f *[mm]*	w_w *[mm]*	t_f *[mm]*	t_w *[mm]*	E_x *[GPa]*	E_y *[GPa]*	ν_{xy}	G_{xy} *[GPa]*	f_x *[MPa]*
A	80	160	8	8	28	10	0.25	3	240
B	100	200	10	10	28	10	0.25	3	240
C	120	240	12	12	28	10	0.25	3	240
D	150	300	15	15	28	10	0.25	3	240

Table 2. Dimensions and mechanical properties of the analyzed beams.

Note that commercial “I” profiles here considered present overall depth and thickness respectively equal to twice and 1/10 flange width.
More specifically the values of the critical uniformly distributed load, associated to the local buckling, through the proposed mechanical model are calculated, by varying the following geometrical parameter:

$$SF = \frac{w_w}{w_f t_f}l. \tag{13}$$

Furthermore, in order to characterizes the local to global buckling transition, a mechanical model formulated from the same authors is used [6].
In Figure 5, the ratio between the bending moment in mid span cross-section due to critical transverse load and the ultimate flexural moment versus *SF* is plotted.

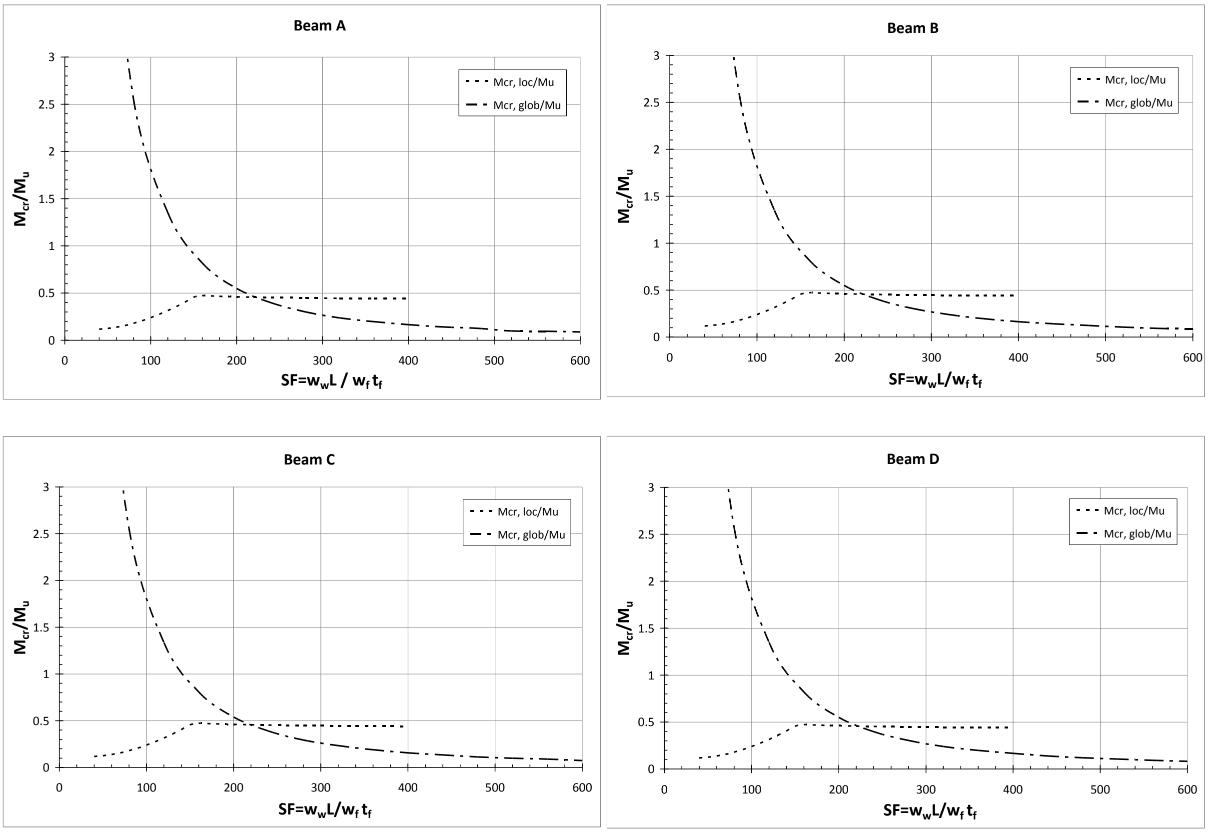

Figure 5. Buckling curves for the analyzed beams.

6 Conclusions

A mechanical model capable to take into account the shear deformability of the composite material on the local buckling behavior of pultruded FRP thin-walled beams and columns has been proposed.
The buckling behavior of some "I" simply supported beams has been investigated by means of a finite element approximation.
The results have shown that:

- the ratio between the bending moment in mid span cross-section due to buckling transverse load and the ultimate flexural moment over the *SF* parameter assumes the same value for all the investigated beams (Figure 6);
- the values of the transverse load corresponding to buckling collapse are lower than 50% of that corresponding to the ultimate bending moment of the analyzed beams.

The numerical analyses have also highlighted that the local buckling mode is characterized by web or flange crisis depending on beam slenderness.
More specifically, the web to flange buckling transitions occurs for a value of *SF* approximately equal to 150.

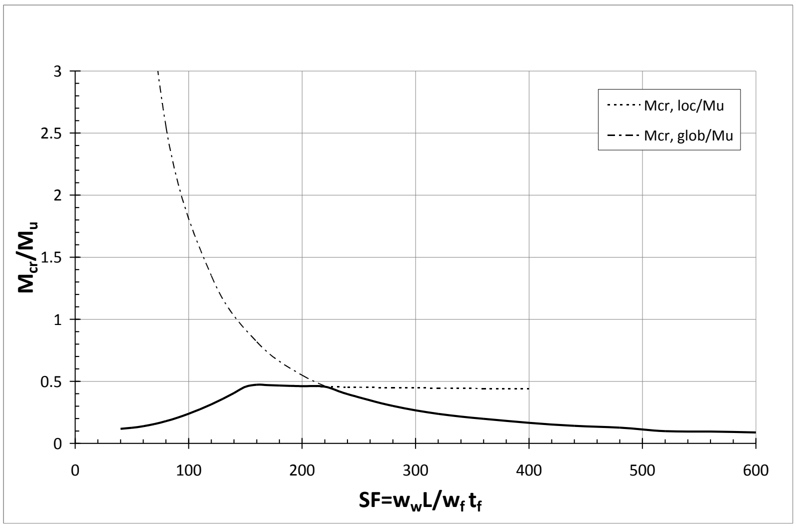

Figure 6. Buckling curves for I beams.

References

[1] SAADÈ K, ESPION B, WARZÈE G. Non-uniform torsional behavior and stability of thin-walled elastic beams with arbitrary cross-sections. *Thin-Walled Structures* 2004;42:857–81.

[2] DE LORENZIS L, LA TEGOLA A. Effect of the actual distribution of applied stresses on global buckling of isotropic and transversely isotropic thin-walled members: theoretical analysis. *Composite Structures* 2005;68:339–48.

[3] TURVEY GJ, ZHANG Y. A computational and experimental analysis of buckling, postbuckling and initial failure of pultruded GRP columns. *Comput Struct* 2006;84:1527–37.

[4] ROBERTS T.M., AL-UBAIDI, H., "Influence of shear deformation on restrained torsional warping of pultruded FRP bars of open cross-section". *Thin-Walled Structures*, V. 39, 2001, pp. 395-414.

[5] ROBERTS, T.M., "Influence of shear deformation on buckling of pultruded fiber reinforced plastic profiles". *Journal of Comp. Constr.*, V. 6 N. 4, 2002, pp. 241–248.

[6] ASCIONE, L., GIORDANO, A., SPADEA, S., "Lateral buckling of pultruded FRP beams", *Composites: Part B*, V.42 N.4, 2011, pp 819-824.

[7] FEO L, MANCUSI G. "Modeling shear deformability of thin-walled composite beams with open cross-section". *Mech. Research Commun.* 2010, V.37, N.3, pp. 320-325.

[8] CNR DT-205/2006, "Guide for the design and construction of structures made of FRP pultruded elements", *Italian National Research Council (CNR) Ed.*, 2006.

[9] MOSALLAM, A.S., ELSADEK, A.A., PUL, S., "Semi-Rigid Behavior Of Web-Flange Junctions Of Open-Web Pultruded Composites", *Proceedings of the International Conference on FRP Composites*, San Francisco, California, Nov. 4-6, 2009.

[10] QIAO, P., SHAN, L., "Explicit local buckling analysis and design of fiber-reinforced plastic composite structural shapes", *Composites Structures*, V. 70, 2005, pp. 468-483.

[11] QIAO, P., SHAN, L., "Explicit local buckling analysis of rotationally restrained composites plates under uniaxial compression", *Eng. Structures* 2008, V.30, pp.126-140.

[12] REISSNER, E., "The effect of transvers shear deformation on the bending of elastic plates", *J. Math. Phys*. V. 12, 1945.

[13] MINDLIN, R.D., "Infuence of rotatory inertia and shear deformation on flexural motions of isotropic elastic plates", *J. Appl. Mech*., V. 18, 1951.

[14] COMO M., GRIMALDI, A., "Theory of stability of continuous elastic structures", *CRC Press* (1995).

[15] REDDY, J.N., "An introduction to finite element method", *McGraw Hill, Singapore* 2006.

[16] BANK, L.C., YIN, J., "Buckling of orthotropic plates with free and rotationally restrained unloaded edges", *Thin Walled Structures*, V. 24, 1996, pp. 83-96.